Dynamic-Feature Extraction, Attribution, and Reconstruction (DEAR) Method for Power System Model Reduction

Shaobu Wang, *Member, IEEE*, Shuai Lu, *Senior Member, IEEE*, Ning Zhou, *Senior Member, IEEE*, Guang Lin, *Member, IEEE*, Marcelo Elizondo, *Member, IEEE*, and M. A. Pai, *Life Fellow, IEEE*

***Abstract*—In interconnected power systems, dynamic model reduction can be applied to generators outside the area of interest (i.e., study area) to reduce the computational cost associated with transient stability studies. This paper presents a method of deriving the reduced dynamic model of the external area based on dynamic response measurements. The method consists of three steps, namely dynamic-feature extraction, attribution, and reconstruction (DEAR). In this method, a feature extraction technique, such as singular value decomposition (SVD), is applied to the measured generator dynamics after a disturbance. Characteristic generators are then identified in the feature attribution step for matching the extracted dynamic features with the highest similarity, forming a suboptimal "basis" of system dynamics. In the reconstruction step, generator state variables such as rotor angles and voltage magnitudes are approximated with a linear combination of the characteristic generators, resulting in a quasi-nonlinear reduced model of the original system. The network model is unchanged in the DEAR method. Tests on several IEEE standard systems show that the proposed method yields better reduction ratio and response errors than the traditional coherency based reduction methods.**

***Index Terms*—Dynamic response, feature extraction, model reduction, orthogonal decomposition, power systems.**

NOMENCLATURE

t	Time.
δ	Rotor angle of synchronous machine.
ω	Rotor speed of synchronous machine.
P_m	Mechanical power.
P_e	Electrical power.
H	Inertia constant of synchronous machine.
D	Damping ratio of synchronous machine.
D_g	Degree of characteristic generators in the super set.
J	Metric for response error.
$\boldsymbol{x}$	Optimal orthogonal bases.
$\hat{\boldsymbol{s}}$	Approximation using optimal orthogonal bases.
ξ	Set of characteristic generators.
$\overline{\xi}$	Set of rotor angles of non-characteristic generators.
T	Coefficient matrix between $\boldsymbol{x}$ and $\hat{\boldsymbol{s}}$.
m	Dimensionality of original space.
r	Dimensionality of reduced space.
K	First r columns of $\boldsymbol{T}$.
C	Coefficient matrix connecting $\overline{\xi}$ and ξ.
R	Reduction ratio.

Manuscript received March 26, 2013; revised July 19, 2013, November 06, 2013, and January 06, 2014; accepted January 12, 2014. Date of publication January 31, 2014; date of current version August 15, 2014. This work was supported by the Advanced Scientific Computing Research (ASCR) program of the U.S. Department of Energy (DOE) Office of Science. Pacific Northwest National Laboratory is operated by Battelle for DOE under Contract DE-AC05-76RL01830. Paper no. TPWRS-00370-2013.

S. Wang, S. Lu, N. Zhou, G. Lin, and M. Elizondo are with Pacific Northwest National Laboratory, Richland, WA 99352 USA (e-mail: shaobu.wang@pnnl.gov; shuai.lu@pnnl.gov; ning.zhou@pnnl.gov; guang.lin@pnnl.gov; marcelo.elizondo@pnnl.gov).

M. A. Pai is with the Department of Electrical and Computer Engineering, University of Illinois at Urbana-Champaign, Urbana, IL 61801 USA (e-mail: mapai@illinois.edu).

Color versions of one or more of the figures in this paper are available online at http://ieeexplore.ieee.org.

Digital Object Identifier 10.1109/TPWRS.2014.2301032

I. INTRODUCTION

IN interconnected power systems, dynamic model reduction (DMR) for generators outside the area of interest has been investigated to reduce the expensive computational cost of transient stability studies [1]–[15]. DMR holds promise to represent the real system with proper degrees of approximation while maintaining relevant dynamic properties, which enables faster simulations of system responses to disturbances. Successful implementation of DMR is critical for online dynamic security assessments in which many scenarios need to be considered as part of contingency analysis. This approach ensures outage prevention and outage recovery where strategic islanding may be necessary to assure dynamic stability in real-time, wide-area control and protection.

DMR generally consists of identifying and aggregating generators to be reduced, followed by reconfiguring the network model [16]. "Coherency" is the most common concept adopted in the identification step. Coherency has the advantage of retaining the physical structure of the system compared to other means, such as the technique known as "model equivalencing" [2], [3]. Depending on the methods used to identity a group, coherency-based reduction techniques can be classified into three types, which are described below.

Type I relies on analyzing linearized models of systems around an operating point. When grid topology changes (e.g., lines are tripped) following a large disturbance, the identification results obtained for the pre-fault system may not be valid

for the post-fault system. Type II identifies coherency groups by analyzing the results of offline dynamic simulations. These methods are more reliable and usually yield a higher reduction ratio; but the resulting reduced model has very limited applicability in real time because both the system topology and operation point will be different from the offline studies. Type III methods rely on online measurements and computation, taking advantage of advanced hardware, including phasor measurement units, broadband communications, and fast computers, and with the potential to address issues associated with the other approaches.

Coherency-based methods can perform well if most generators only have strong participation in local oscillation modes. However, coherency can be blurred when multiple inter-area modes exist, resulting in performance deterioration (in terms of reduction ratios and response errors) by the coherency-based reduction methods. Most coherency methods for model reduction also do not consider voltage variations on the coherency generators, as pointed out by Joo *et al.* [14].

In this paper, a new DMR method is proposed. Similar to the Type III methods, the proposed method is based on dynamic phasor measurement data of generators, but attempts to avoid the weaknesses of coherency identification. The proposed method is composed of the three steps: dynamic-feature extraction, attribution, and reconstruction (DEAR). In the extraction step, a feature extraction technique, such as singular value decomposition (SVD), is applied to the measured generator dynamics following a disturbance. In the feature attribution step, characteristic generators that have responses matching the extracted features (e.g., the orthogonal components from SVD) with the highest similarity are then identified. Characteristic generators form a suboptimal "basis" of system dynamics. In the reconstruction step, all generator state variables, such as rotor angles and voltage magnitudes, are approximated with a linear combination of the characteristic generators. Non-characteristic generators are thus eliminated from numerical integration. The characteristic generator set usually contains a much smaller number of machines than the original system, and can be adjusted to meet the accuracy requirement.

The system derived from the proposed DEAR method is a quasi-nonlinear reduced model of the original system, in the sense that the nonlinear properties of the characteristic generators and the network are still retained while the nonlinear dynamics of other generators are eliminated. The accuracy in approximating the original system would be acceptable for a wider range of operating points compared to reduction approaches based on model linearization. Another advantage of the DEAR method is that the network model is unchanged in the reduced model, which simplifies the model reduction process compared to most coherency-based approaches. Retaining the original network model also allows for specific generators outside the characteristic generator set to remain in the reduced model if so desired. These properties make the online DMR using the DEAR method much more convenient and flexible.

II. Application of Dynamic Model Reduction

NERC standards require that transmission operators maintain reliable operation of the system under the most severe single contingency [24]. In the NERC studies, the model of the entire interconnection[1] is used, with more detailed information of a transmission company's own system (called the internal area or the study area), but less detailed modeling is conducted for the rest of the transmission network (called the external area). Because the planning studies are performed on offline models, a number of assumptions have to be made as to the status of transmission lines and devices, generator dispatch patterns, and loads at each bus. Real-time system conditions are often quite different from these assumptions and sometimes render the results of the planning studies inapplicable. To overcome this problem, many transmission operators perform online transmission analyses to achieve faster evaluation of reliability and produce corrective strategies.

Stability studies are the most time-consuming of all types of transmission studies and are part of the extensive dynamic security assessment (DSA). In online and offline applications involving stability studies, DMR can be performed on the model of the external area to reduce the computational burden. A large number of control and protection schemes responding a disturbance can be tested in the study area with a reduced external area model, thus improving the efficiency of both planning and operation of the transmission network.

The goal of DMR is to reduce the number of variables and equations used to represent the external area as much as possible, while keeping the responses of internal generators and other relevant devices unchanged to the degree possible. Descriptions of the proposed DEAR method for DMR and validation of its effectiveness on IEEE standard test systems are discussed in the rest of this paper.

III. DEAR Method for Dynamic Model Reduction

A. Basic Idea

Application of the method to larger systems and higher-order machine models are discussed later in this section. For clarity, the classical model for a three-machine system shown in (1) is used as an example to describe the basic idea:

$$\begin{cases} \frac{d\delta_1}{dt} = (\omega_1 - 1)\omega_s \\ \frac{d\omega_1}{dt} = \frac{[P_{m1} - P_{e1} - D_1(\omega_1 - 1)]}{(2H_1)} \\ \frac{d\delta_2}{dt} = (\omega_2 - 1)\omega_s \\ \frac{d\omega_2}{dt} = \frac{[P_{m2} - P_{e2} - D_2(\omega_2 - 1)]}{(2H_2)} \\ \frac{d\delta_3}{dt} = (\omega_3 - 1)\omega_s \\ \frac{d\omega_3}{dt} = \frac{[P_{m3} - P_{e3} - D_3(\omega_3 - 1)]}{(2H_3)}. \end{cases} \tag{1}$$

Fig. 1 shows the rotor angles of generators, δ_1, δ_2, and δ_3, after disturbance.

As the first step, the dynamic feature of this simple system is identified, which has only one oscillation frequency and speed of decay. In the second step, generator G1 is selected as the characteristic generator because its dynamics are quite representative (we do this by observation in this simple example). In the third step, the angle variable δ_1 is used to represent δ_2 and δ_3. In fact, δ_1, δ_2, and δ_3 satisfy the relation in

$$\begin{cases} \delta_2 \approx \alpha\delta_1 \\ \delta_3 \approx \beta\delta_1 \end{cases} \tag{2}$$

[1]The transmission planning coordinator is responsible for maintaining the model for the entire interconnection and improving its accuracy. For example, the Western Electricity Coordinating Council performs this function in the Western interconnection.

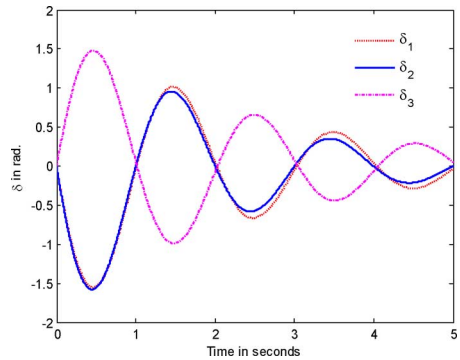

Fig. 1. Illustration of rotor angle dynamics in a three-machine system.

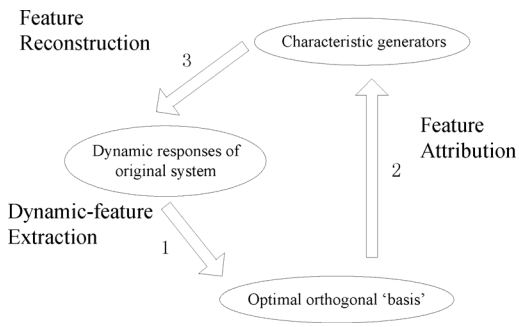

Fig. 2. Diagram of the DEAR method.

where $\alpha \approx 1$, $\beta \approx -1$ are constants and will be evaluated through (21). Ignoring errors represented by "$\approx$" in (2) and inserting it into (1), the original system can be simplified as (3):

$$\begin{cases} \frac{d\delta_1}{dt} = (\omega_1 - 1)\omega_s \\ \frac{d\omega_1}{dt} = \frac{[P_{m1} - P_{e1} - D_1(\omega_1 - 1)]}{(2H_1)} \\ \delta_2 = \alpha\delta_1 \\ \delta_3 = \beta\delta_1. \end{cases} \tag{3}$$

Four differential equations were eliminated in (3) compared to (1) for this simple example. The network model will be kept the same when performing numerical integration for the system because no aggregation is needed in the reduction of generator state variables. We follow the same procedure for the DMR of generators in larger systems, as described in detail below and illustrated in Fig. 2:

Step 1) Dynamic-feature extraction—Analyze the dynamic response vectors of the original system for a disturbance, and find the optimal orthogonal bases of these responses.

Step 2) Feature attribution—Identify generators with responses that are highly similar to the optimal orthogonal bases and designate those units as the characteristic generators.

Step 3) Feature reconstruction—Use linear combinations of the characteristic generators to approximate non-characteristic generators.

B. Dynamic-Feature Extraction: Finding the Optimal Orthogonal Bases

In this subsection, we discuss the concept of optimal orthogonal bases of a system's dynamic responses and how to identify them.

For convenience, the classical generator model is assumed, and rotor angles, δ, are the state variables. The magnitude of the generator internal voltage, E', is assumed to be constant.

Suppose $\delta_1, \delta_2, \ldots, \delta_i, \ldots, \delta_m$ are the m rotor angles of the system to be reduced. The term $\boldsymbol{\delta_i}$ is an n-dimensional row vector representing the dynamic of rotor angle δ_i following a disturbance. Its elements are time series: $\delta_i(t_1), \delta_i(t_2), \ldots, \delta_i(t_n)$.

Define

$$\boldsymbol{\delta} = [\boldsymbol{\delta_1}; \boldsymbol{\delta_2}; \ldots; \boldsymbol{\delta_m}]. \tag{4}$$

Here, $\boldsymbol{\delta}$ is an $m \times n$ matrix. Suppose $\boldsymbol{x} = [\boldsymbol{x_1}; \boldsymbol{x_2}; \ldots; \boldsymbol{x_i}; \ldots; \boldsymbol{x_r}]$ is the set of optimal orthogonal bases. Here, $r < m$, and $\boldsymbol{x_i}$ is an n-dimensional row vector. "Optimal" means that for any $r < m$, $\boldsymbol{\delta_i}$ can be approximated by a linear combination of $\boldsymbol{x}$, and the errors between the approximation, $\hat{\boldsymbol{s}}$, and the actual responses are minimized. In other words, given any $r < m$, we need to find an optimal $\boldsymbol{x}$, such that

$$\hat{\boldsymbol{s}} = \boldsymbol{K}\boldsymbol{x} \tag{5}$$

where $\boldsymbol{K}$ is an $m \times r$ matrix, and

$$\|\boldsymbol{\delta} - \hat{\boldsymbol{s}}\|_2 = \sum_{i=1}^{m} (\boldsymbol{\delta}_i - \hat{\boldsymbol{s}}_i)^{\mathrm{T}} (\boldsymbol{\delta}_i - \hat{\boldsymbol{s}}_i) \tag{6}$$

is minimized.

In this paper, we adopt the SVD algorithm to solve the above problem. Through SVD we get

$$\boldsymbol{\delta} = \boldsymbol{U}\boldsymbol{D}\boldsymbol{W}^{\mathrm{T}} \tag{7}$$

where $\boldsymbol{U}$ is an $m \times m$ unitary matrix, $\boldsymbol{D}$ is an $m \times n$ rectangular diagonal matrix with nonnegative real numbers on the diagonal, and $\boldsymbol{W}^{\mathrm{T}}$ is an $n \times n$ unitary matrix. The first r[2] rows of $\boldsymbol{W}^{\mathrm{T}}$ constitute the optimal orthogonal bases, which can be used to approximate $\boldsymbol{\delta}$. The diagonal elements of $\boldsymbol{D}$ (i.e., singular values of $\boldsymbol{\delta}$) in descending order are scaling factors indicating the strength or energy of the corresponding row vectors of $\boldsymbol{W}^{\mathrm{T}}$.

Define

$$\begin{aligned} \boldsymbol{x} &= \boldsymbol{W}^{\mathrm{T}}(1:r,:) \\ \boldsymbol{K} &= \boldsymbol{T}(:,1:r) \end{aligned} \tag{8}$$

where $\boldsymbol{T} = \boldsymbol{U}\boldsymbol{D}$; $\boldsymbol{K}$ is the first r columns of $\boldsymbol{T}$. As a result, $\boldsymbol{\delta}$ can be approximated by $\hat{\boldsymbol{s}} = \boldsymbol{K}\boldsymbol{x}$. For any $r < m$, the SVD algorithm can guarantee that (6) is minimized.

Remark 1: Although there may exist thousands of modes in the mathematic model of a large-scale power system, usually only a small fraction of them are noticeably excited by a disturbance. We refer to these modes as "dominant modes," and the rest as "dormant modes". Usually, "dominant modes" have strong oscillation energy (shown as the "features" in system dynamics), while "dormant modes" have weak energy and are hard to observe. Here, SVD is used to extract the features composed of those "dominant modes," which correspond to the first r diagonal elements of matrix D in (7), unlike how it is used in traditional linear system model reduction methods (e.g., balanced

[2]The value r is selected according to the accuracy requirement in the reduced model. Larger r values result in lower reduction ratios but a more accurate approximation of the original system and vice versa.

truncation [19] or Hankel norm reduction [20]). More details about the SVD algorithm can be found in Berrar *et al.* [21] and Antoulas [22].

C. Feature Attribution: Determine Characteristic Generators

The r optimal orthogonal basis vectors found in the feature extraction step will result in minimal errors when used to approximate $\boldsymbol{\delta}$. If each of these basis vectors exactly matches the dynamic angle response of one of the generators, then the angle dynamics of the other generators must have very minimal energy impact (because their corresponding singular values are smaller). This means we can just keep these r generators in the model and ignore the other generators. Although this will not happen in a real system because generators usually participate in multiple oscillation modes, we still will try to match an optimal basis with the generator whose dynamic response has the highest similarity to this "oscillation pattern," and will call the generator a characteristic generator. We then will use the set of characteristic generators as sub-optimal bases to represent the entire system.

To determine the characteristic generators, we need to find a subset of $\boldsymbol{\delta} = [\boldsymbol{\delta}_1; \boldsymbol{\delta}_2; \ldots; \boldsymbol{\delta}_m]$ such that this subset has the highest similarity to $\boldsymbol{x}$, the optimal orthogonal set. In other words, we need to find

$$\boldsymbol{\xi} = [\underbrace{\boldsymbol{\delta}_p; \boldsymbol{\delta}_q; \cdots; \boldsymbol{\delta}_z}_{r}] \tag{9}$$

such that $\boldsymbol{\xi}$ is highly similar to $\boldsymbol{x}$.

According to the last subsection, any $\boldsymbol{\delta}_q$ can be approximated by a linear combination of the optimal orthogonal bases:

$$\begin{aligned} \boldsymbol{\delta}_p &\approx \boldsymbol{K}_{p1}\boldsymbol{x}_1 + \boldsymbol{K}_{p2}\boldsymbol{x}_2 + \cdots + \boldsymbol{K}_{pi}\boldsymbol{x}_i + \cdots + \boldsymbol{K}_{pr}\boldsymbol{x}_r \\ &\vdots \\ \boldsymbol{\delta}_q &\approx \boldsymbol{K}_{q1}\boldsymbol{x}_1 + \boldsymbol{K}_{q2}\boldsymbol{x}_2 + \cdots + \boldsymbol{K}_{qi}\boldsymbol{x}_i + \cdots + \boldsymbol{K}_{qr}\boldsymbol{x}_r. \end{aligned} \tag{10}$$

Here, $\boldsymbol{x}$ is the optimal orthogonal basis and $\boldsymbol{\delta}$ is normalized [8]. A larger $|\boldsymbol{K}_{qi}|$ indicates a higher degree of co-linearity between the two vectors ($\boldsymbol{\delta}_q$ and $\boldsymbol{x}_i$). For example, if $|\boldsymbol{K}_{qi}| > |\boldsymbol{K}_{pi}|$, it indicates that the similarity between $\boldsymbol{x}_i$ and $\boldsymbol{\delta}_q$ is higher than that between $\boldsymbol{x}_i$ and $\boldsymbol{\delta}_p$. $\boldsymbol{\delta}_q$ will have the highest similarity to $\boldsymbol{x}_i$, if the inequality in (11) holds:

$$|\boldsymbol{K}_{qi}| > |\boldsymbol{K}_{pi}|, \text{ for } \forall\, p \in \{1, 2, \ldots, m\},\ p \neq q. \tag{11}$$

By doing so, a rotor angle response of the highest similarity can be identified for each optimal orthogonal basis. As a result, $\boldsymbol{\xi}$ in (9) is determined.

Remark 2: The same characteristic generator can appear two or more times in (9) when using the criteria in (11). For example, if $\boldsymbol{\delta}_q$ has the highest similarity to both $\boldsymbol{x}_i$ and $\boldsymbol{x}_j$, then we will have two $\boldsymbol{\delta}_q$ entries in (9). In that case, delete one of the entries, and thus, $r = r - 1$.

Remark 3: From an engineering perspective, some generators may be of particular interest, and detailed information about them is preferred. Dynamic equations for these generators can be kept in the reduced model without being approximated if they are not identified as characteristic generators.

D. Feature Reconstruction: Model Reduction Using the Linear Combination of Characteristic Generators

According to (7)–(10), $\boldsymbol{\delta}$ can now be arranged as (12):

$$\boldsymbol{\delta} = \begin{bmatrix} \boldsymbol{\xi} \\ \overline{\boldsymbol{\xi}} \end{bmatrix} \approx \begin{bmatrix} \boldsymbol{K}_{\xi} \\ \boldsymbol{K}_{\overline{\xi}} \end{bmatrix} \boldsymbol{x} \tag{12}$$

where $\boldsymbol{\delta}$ is an $m \times n$ matrix defined in (4), $\boldsymbol{\xi}$ is an $r \times n$ matrix defined in (9) representing rotor angle dynamics of characteristic generators, and $\overline{\boldsymbol{\xi}}$ is an $(m-r) \times n$ matrix representing the dynamics of non-characteristic generators; $\boldsymbol{x}$ is an $r \times n$ matrix and can be calculated from (8); and $\boldsymbol{K}_{\xi}$ is an $r \times r$ square matrix; $\boldsymbol{K}_{\overline{\xi}}$ is an $(m-r) \times r$ matrix.

Normally, $\boldsymbol{K}_{\xi}$ is invertible. We have two different approaches to finding the approximate linear relations between $\overline{\boldsymbol{\xi}}$ and $\boldsymbol{\xi}$. The first approach is to solve the following over-determined equation:

$$\overline{\boldsymbol{\xi}} = C\boldsymbol{\xi} \tag{13}$$

where C is an $(m-r) \times r$ matrix and can be determined by the least-squares method, namely, $C = \overline{\boldsymbol{\xi}}\left[\left(\boldsymbol{\xi}\,\boldsymbol{\xi}^{\mathrm{T}}\right)^{-1}\boldsymbol{\xi}\right]^{\mathrm{T}}$. Another approach is to use the approximate linear relations in (12). According to (12), we have

$$\boldsymbol{\xi} \approx \boldsymbol{K}_{\xi}\boldsymbol{x} \tag{14}$$

and

$$\overline{\boldsymbol{\xi}} \approx \boldsymbol{K}_{\overline{\xi}}\boldsymbol{x}. \tag{15}$$

Pre-multiplying $\boldsymbol{K}_{\xi}^{-1}$ on both sides of (14) yields

$$\boldsymbol{x} \approx \boldsymbol{K}_{\xi}^{-1}\boldsymbol{\xi}. \tag{16}$$

Substituting (16) into (15) yields

$$\overline{\boldsymbol{\xi}} \approx \boldsymbol{K}_{\overline{\xi}}\boldsymbol{K}_{\xi}^{-1}\boldsymbol{\xi}. \tag{17}$$

Equation (13) or (17) establishes the approximate linear relations between the rotor angle dynamics of characteristic generators and that of non-characteristic generators. The dynamics of all generators in the original system then can be reconstructed by using only the dynamic responses from characteristic generators.

E. Generalization to High Order Models

In classical models, it is assumed that the magnitude of the generator internal voltage E' is constant, and only its rotor angle δ changes after a disturbance. In reality, with the generator excitation system, E' also will respond dynamically to the disturbance. The dynamics of E' can be treated in the same way as rotor angle δ in the DEAR method to improve the reduced model, except that the set of characteristic generators needs to be determined from δ. This way, both δ and E' of non-characteristic generators will be represented in the reduced model using those of the characteristic generators.

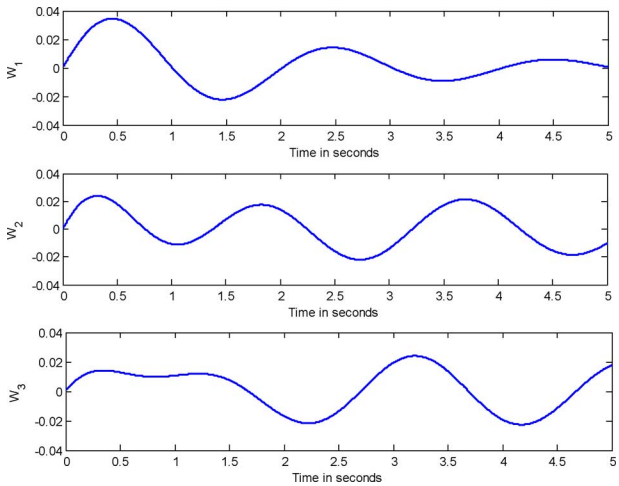

Fig. 3. Extracted dynamic features in the three-machine system.

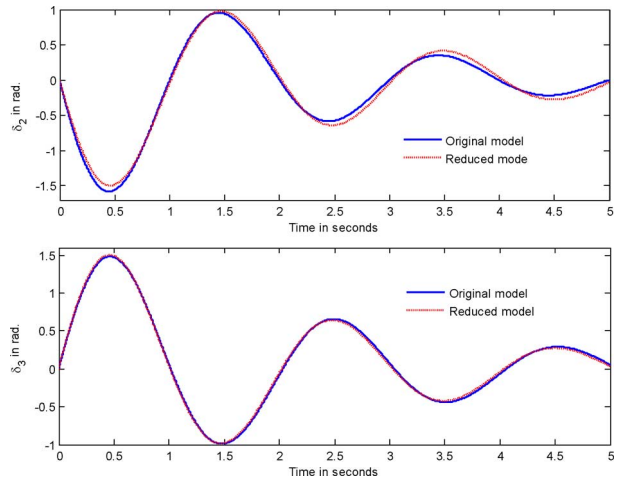

Fig. 4. Actual and reconstructed rotor dynamics of δ_2 and δ_3.

F. Online Application of the DEAR Method

For offline studies, the DEAR process can be performed at different conditions and operating points of the target system (external area) to obtain the corresponding reduced models. For online applications, however, computational cost may be very high if SVD has to be calculated every time the system configuration changes. A compromise can be made by maintaining a fixed set of characteristic generators, which is determined by doing SVDs for multiple scenarios offline and taking the super-set of the characteristic generators from each scenario. During real-time operation of the system, the approximation matrix C from (13) used for feature reconstruction is updated (e.g., using the recursive least-square method) based on a few seconds' data right after a disturbance. This way, SVD is not needed every time after a different disturbance occurs.

IV. Case Studies

A. Case 1

First, we test the proposed approach on the simple three-machine system in (1), which has the angle dynamics δ_1, δ_2, and δ_3 shown in Fig. 1.

1) Dynamic-Feature Extraction: Let $\boldsymbol{\delta} = [\boldsymbol{\delta}_1, \boldsymbol{\delta}_2, \boldsymbol{\delta}_3]^{\mathrm{T}}$. Using (7), we obtain $\boldsymbol{W}_1 = \boldsymbol{W}^{\mathrm{T}}(1,:)$, $\boldsymbol{W}_2 = \boldsymbol{W}^{\mathrm{T}}(2,:)$, and $\boldsymbol{W}_3 = \boldsymbol{W}^{\mathrm{T}}(3,:)$, which are shown in Fig. 3. The relationship between $\boldsymbol{\delta}$ and $\boldsymbol{W}$ is

$$\begin{bmatrix} \boldsymbol{\delta}_1 \\ \boldsymbol{\delta}_2 \\ \boldsymbol{\delta}_3 \end{bmatrix} = \begin{bmatrix} T_{11} & T_{12} & T_{13} \\ T_{21} & T_{22} & T_{22} \\ T_{31} & T_{32} & T_{33} \end{bmatrix} \begin{bmatrix} \boldsymbol{W}_1 \\ \boldsymbol{W}_2 \\ \boldsymbol{W}_3 \end{bmatrix} \tag{18}$$

where

$$\boldsymbol{T} = \begin{bmatrix} -45.5981 & 0.8492 & 0.2486 \\ -43.9095 & -3.0662 & -0.0662 \\ 44.1879 & -2.1705 & 0.1908 \end{bmatrix}$$

and is calculated by $\boldsymbol{T} = \boldsymbol{U}\boldsymbol{D}$.

As can be seen from $\boldsymbol{T}$, the second and third columns of $\boldsymbol{T}$ have much smaller elements than the first column. Therefore, $\boldsymbol{W}_1$ is the most significant dynamic feature of $\boldsymbol{\delta}$. In (8), if we let $r = 1$, then we have

$$\begin{aligned} \boldsymbol{x} &= \boldsymbol{W}_1 \\ \boldsymbol{K} &= \boldsymbol{T}(1:3,1). \end{aligned} \tag{19}$$

2) Feature Attribution: Notice that the three elements of $\boldsymbol{K}$ (i.e., the first column of $\boldsymbol{T}$) are $|-45.5981| > |44.1879| > |-43.9095|$. The generator with $\boldsymbol{\delta}_1$ has the highest similarity to $\boldsymbol{W}_1$ according to (11), and can be chosen as the characteristic generator.

3) Feature Reconstruction: According to (14) and (15), we have

$$\boldsymbol{K}_{\xi} = [-45.5981]; \quad \boldsymbol{K}_{\bar{\xi}} = \begin{bmatrix} -43.9095 \\ 44.1879 \end{bmatrix}. \tag{20}$$

Substituting (20) into (17) yields

$$\begin{bmatrix} \delta_2 \\ \delta_3 \end{bmatrix} = \bar{\boldsymbol{\xi}} \approx \boldsymbol{K}_{\bar{\xi}} \boldsymbol{K}_{\xi}^{-1} \boldsymbol{\xi} = \begin{bmatrix} 0.9630 \\ -0.9691 \end{bmatrix} \delta_1. \tag{21}$$

The reconstructed dynamics of δ_2 and δ_3 are compared to the original data, which are shown in Fig. 4 in which dotted lines represent reconstructed dynamics; solid lines represent original dynamics. It can be seen that $\boldsymbol{\delta}_2$ and $\boldsymbol{\delta}_3$ are restored very well in the reduced model.

B. Case 2

Chow *et al.* compared the performance of different model reduction methods on the NPCC 48-machine system, including Podmore's method, inertial aggregation, slow coherency and optimum aggregation [5]. The DEAR method is applied to this same system to compare with the above methods.

In the NPCC system model [5], generators 1 to 9 comprise the New England system, which is designated to be the internal system, while the other generators comprise the external system. The disturbance is a six-cycle, short-circuit fault that occurs at Medway located outside the Boston area. The disturbance is cleared by removing the line from Medway to Sherman Road. Several reduced models were obtained in [5] by applying different DMR methods. To evaluate performance of these reduced models, Chow *et al.* [5] defined the two metrics shown in (22) and (23), where $\delta_i^f(t)$ and $\delta_i^a(t)$ represent the rotor angle dynamics of generator i obtained from the original system and the

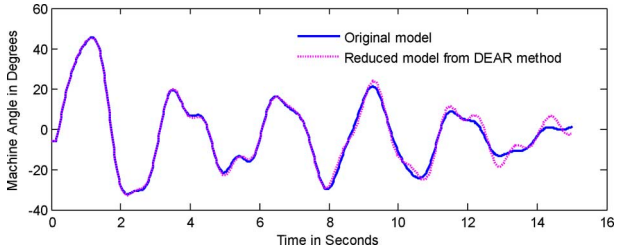

Fig. 5. Time response of machine 1 for the Medway Disturbance.

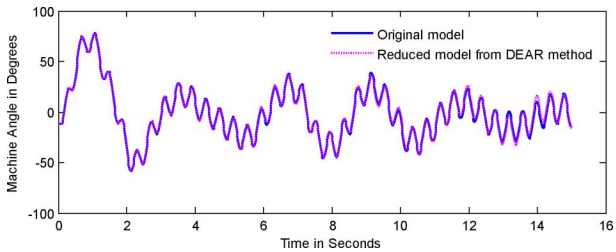

Fig. 6. Time response of machine 4 for the Medway Disturbance.

reduced system, respectively. The performance comparison results are given in Figs. 5 and 6 and [5, Table 2]. Here we evaluate the DEAR method with these same two metrics:

$$J_a(i) = \frac{1}{(t_2 - t_1)} \int_{t_1}^{t_2} |\delta_i^a(t) - \delta_i^f(t)| dt \tag{22}$$

$$J_s(i) = \sqrt{\frac{1}{(t_2 - t_1)} \int_{t_1}^{t_2} \left[\delta_i^a(t) - \delta_i^f(t)\right]^2 dt}. \tag{23}$$

Using the DEAR method, by analyzing rotor angle data in the time interval of $0.15\text{s} < t < 5\text{s}$, generators 10, 23, 24, 25, 29, 30, 36, 39, 40, 41, 43, 44, and 45 are identified as characteristic generators; generator 48 is the reference machine; and the other generators can be removed from the dynamic equations. As a result, 14 machines are maintained in the reduced dynamic model for the external system. Note that the reduced model has the same reduction ratio used by Chow *et al.* [5]. The responses of two internal generators in the study area following the same disturbance are compared between the reduced model and the original model, shown in Figs. 5 and 6, respectively. Solid lines represent the responses of the original model, and dashed lines represent the responses of the reduced model. Performance in terms of differences between the original model's response and that of the reduced model are compared between the DEAR method and the methods in [5, Table 2]. The results are shown in Table I, which suggests the better performance of the DEAR method.

C. Case 3

In this subsection, the IEEE 145-bus, 50-machine system [18] in Fig. 7 is investigated. There are 16 and 34 machines in the internal and external areas, respectively. Generator 37 at Bus 130 in the internal area is chosen as the reference machine. All generators are modeled using classical models. A three-phase, short-circuit fault (F1) is configured on Line 116–136 at Bus

TABLE I
ERROR FUNCTIONS FOR MACHINES 1 AND 4

Reduction Method	$J_a(1)$	$J_s(1)$	$J_a(4)$	$J_s(4)$
Podmore	10.067	13.104	12.648	16.507
Inertial	4.078	5.489	5.218	6.920
Slow Coherency	4.905	6.427	6.272	8.097
Optimum	3.048	4.184	3.800	5.087
DEAR	1.270	1.822	1.035	1.5403

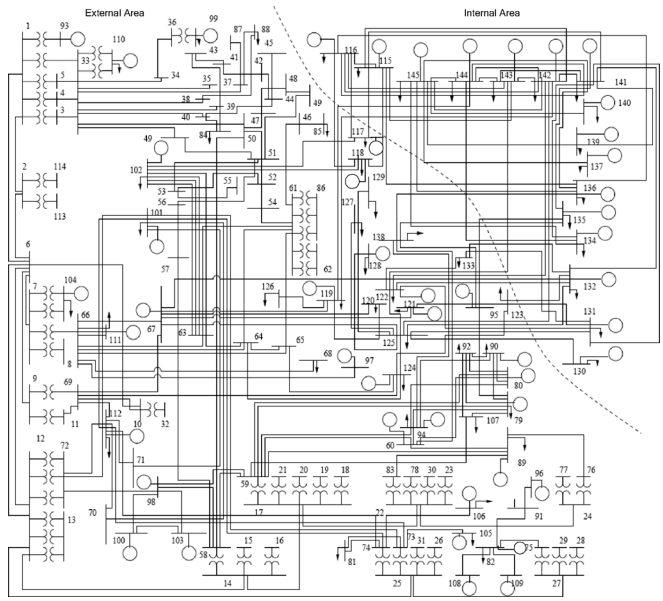

Fig. 7. IEEE 50-machine system.

No. 116 at $t = 1$ s. The fault lasts for 60 ms, and then the line is tripped to clear the fault.

Post-fault rotor angle dynamics in the time interval of $1.2 \leq t \leq 5$ s are analyzed to perform model reduction, using inertial aggregation [5] (one of the coherency-based reduction method) and the DEAR method, so that their performance can be compared.

Many methods are available for coherency identification. In this paper, the principle component analysis method presented by Anaparthi *et al.* [8] and Moore [17] is chosen to identify coherency groups, and the Matlab clustering toolbox is used to aid the analysis. Clustering results according to the rotor angle dynamics in the external area are shown in Fig. 8. In Fig. 8, the horizontal axis represents generator numbers, and the vertical axis scales distances between generator groups. Here the distance is defined in the three-dimensional Euclidean space expanded by the first three columns of the matrix $\boldsymbol{T}$ in (8).

Depending on the distance selected between clusters, different number of coherency groups can be obtained. For example, at a distance larger than 9, two groups are formed (level-2 clustering). Generators 23, 30, and 31 comprise one group, and the other generators comprise another group. Similarly, there are 10 generator groups at level 10, which are shown in the following: Group 1 (generators 30, 31); Group 2 (generator 23); Group 3 (generators 9, 10); Group 4 (generators 16); Groups 5 (generators 7, 13, 15); Group 6 (generator 3); Group 7 (generators 32, 36); Group 8 (generators 8, 18, 25, 33, 34, 35); Group 9 (generators 2, 6); Group 10 (generators 1, 4, 5,

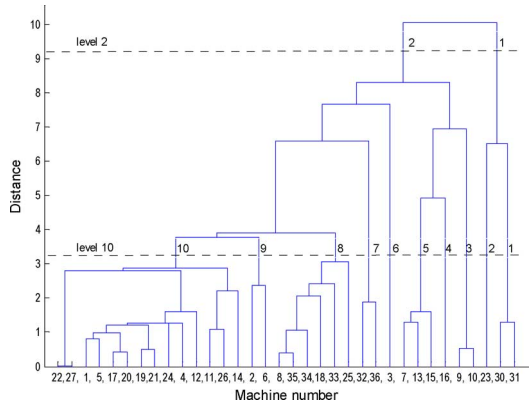

Fig. 8. Coherent groups clustering.

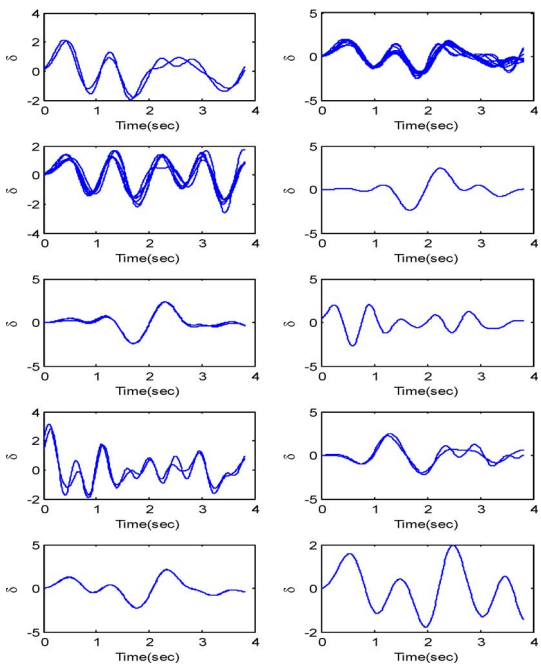

Fig. 9. Dynamic responses of the 10 coherency groups in the IEEE 50-machine system.

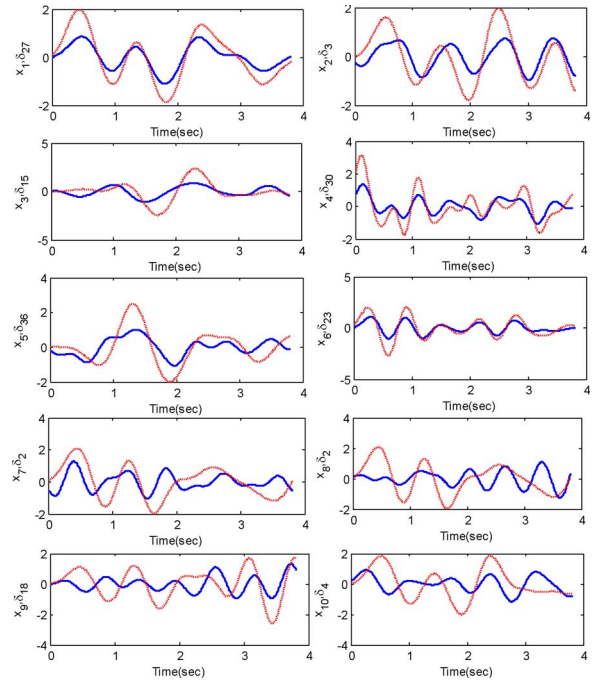

Fig. 10. Optimal orthogonal bases (blue solid lines) and dynamic responses of corresponding characteristic generators (red dashed lines) in the IEEE 50-machine system.

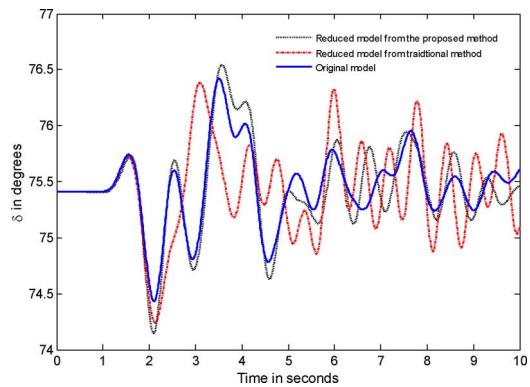

Fig. 11. Rotor angle dynamics of Generator 42 (on Bus 136) following fault F1.

11, 12, 14, 17, 19, 20, 21, 22, 24, 26, 27). Fewer groups result in a simpler system. The normalized (i.e., subtracted by the mean value of the data and divided by its standard deviation) angle dynamics of the 10 groups at level 10 are shown in Fig. 9, where coherency can be observed between generators in the same group. These coherent machines are then aggregated using the inertial aggregation method reported by Chow *et al.* [5]. Finally, we obtain a reduced system with 10 aggregated generators for the external system.

Following the DEAR procedure described in Section III, the optimal orthogonal bases are first obtained by (7) and (8) and by setting $r = 10$. These 10 basis vectors are shown as the blue solid lines in Fig. 10.[3] Then, the corresponding 10 characteristic generators are identified using (11). The rotor angle dynamics of these characteristic generators are shown as dashed red lines in Fig. 10. An approximate linear relation between the characteristic generators and the non-characteristic generators then is established to get the reduced model. Notice that, in this case, $\boldsymbol{\delta}_2$ has the highest similarity to orthogonal bases $\boldsymbol{x}_7$ and $\boldsymbol{x}_8$. Therefore, the set of characteristic generators contains only 9 elements, which is $\boldsymbol{\xi} = [\boldsymbol{\delta}_{27}\, \boldsymbol{\delta}_3\, \boldsymbol{\delta}_{15}\, \boldsymbol{\delta}_{30}\, \boldsymbol{\delta}_{36}\, \boldsymbol{\delta}_{23}\, \boldsymbol{\delta}_2\, \boldsymbol{\delta}_{18}\, \boldsymbol{\delta}_4]^{\mathrm{T}}$.

With the reduced models developed using both coherency aggregation and the DEAR method, the performance of these two methods can be compared. Under the forgoing disturbance, the dynamic response of generator G42 (connected to the faulted line) from these two reduced models and from the original model are shown in Fig. 11.

The blue solid line is from the original model. The red dashed-dotted line is from the reduced model by coherency aggregation, and the black dotted line is by the DEAR method. The reduced model by the DEAR method appears to have smaller differences from original model, and outperforms the coherency aggregation method.

[3]To compare the similarity on the same scales, the amplitudes of the optimal orthogonal bases are multiplied by 10 when shown in Fig. 10.

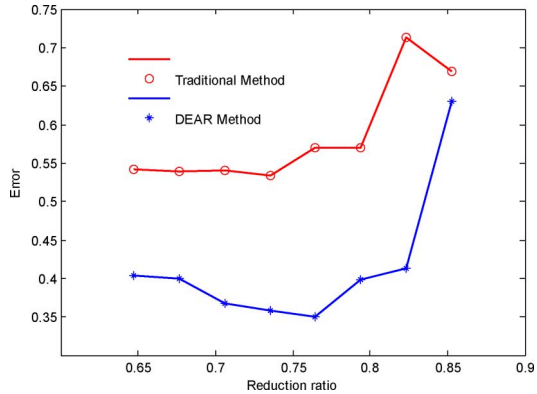

Fig. 12. Performance comparison between the coherency aggregation method and the proposed DEAR method.

Another important metric for evaluating the performance of model reduction is the reduction ratio, which is defined as

$$R = \frac{(N_{\mathrm{F}} - N_{\mathrm{R}})}{N_{\mathrm{F}}} \tag{24}$$

where N_{R} is the total number of state variables of the reduced model of the external system and N_{F} is that of the original model.

Using the metric in (23), the mismatch between the black dotted line and the blue solid line in Fig. 11 is 0.1630, and the reduction ratio defined by (24) is $R = (34-9)/34 = 0.7353$, both of which represent the performance of the proposed method. The mismatch between the red dashed-dotted line and the blue solid line in Fig. 11 is 0.4476 and $R = (34-10)/34 = 0.7059$, both representing the performance of the coherency aggregation method. Therefore, it can be concluded that the proposed method performs better under the metric defined in (23), even under a slightly higher reduction ratio.

We now investigate if the same conclusion can be drawn under different reduction ratios and for generators other than G42 shown in Fig. 11.

Define a comprehensive metric shown in (25) for all the internal generators. Here, φ is the set of all the generators in the internal system; and N is the total number of these generators:

$$J = \frac{1}{N}\sum_{i\in\varphi} J_s(i). \tag{25}$$

A performance comparison of the proposed method and the traditional coherency aggregation is shown in Fig. 12, in which the horizontal axis represents the reduction ratio defined in (24), and the vertical coordinates represent the error defined in (25). It is apparent that the proposed DEAR method consistently performs better than the coherency method.

To demonstrate the basic idea of a super set of characteristic generators in Section III-F, three faults (three-phase fault lasting for 60 ms) are configured on Line 116–136, Line 116–143 and Line 115–143, respectively. Choose the size r of the characteristic generator set for each fault scenario to be 9 here. Define D_g as the number of times each generator appears as a characteristic generator after analyzing the system dynamic response to a fault. For example, Generator 2 is a characteristic generator in all the three fault scenarios; it, therefore, has a D_g of 3. D_g of each characteristic generator is shown in Table II.

TABLE II
D_g OF CHARACTERISTIC GENERATORS

D_g	3	3	3	3	3	2	2	2	2	1	1	1	1
Gen. no.	2	15	18	23	30	3	4	22	36	11	27	31	32

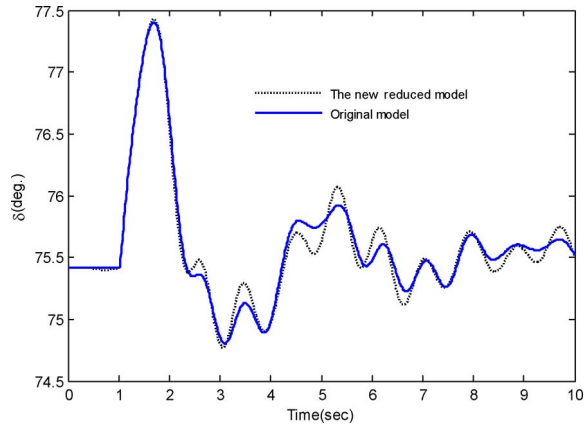

Fig. 13. Rotor angle dynamics of Generator 42 (on Bus 136) following fault F4.

Select $D_g = 2$ as a threshold, i.e., generators with $D_g \geq 2$ are chosen to form the super set of characteristic generators. The following generators are selected: generator 2, 15, 18, 23, 30, 3, 4, 22, and 36.

With the super set, three different coefficient matrices C in (13) can be obtained for the three faults, denoted by C_1, C_2, and C_3. Then a rough estimation of a generalized C can be obtained by, e.g., letting $C_g = (C_1 + C_2 + C_3)/3$. When another three phase fault takes place, for example, F4 on Line 141-143, measurement data for the first three seconds after fault clearance can be used to refine the coefficient matrix C_g. Applying the recursive least square method, C_g is replaced by the more accurate coefficients in C_4. We thus get a new reduced model, represented by the super set of characteristic generators and the coefficient matrix C_4, without performing SVD. The performance of the new reduced model is illustrated in Fig. 13 using the rotor dynamics of Generator 42.

D. Case 4

Pyo *et al.* [23] present a coherency aggregation method that can handle higher-order models with excitation systems, and apply the method using the IEEE 39-bus system. Here the DEAR method is applied on the same system to compare the performance.

In the IEEE 39-bus system [23] shown in Fig. 14, there are four and six generators in the internal and the external area, respectively. In [23], four machines remain in the external system after reduction (G2 at Bus 31 and G3 at Bus 32 are aggregated; G4 at Bus 33 and G5 at Bus 34 are aggregated). After a three-phase fault at Bus 2, which lasts 100 ms and is cleared by removing the line between Bus 2 and Bus 3, the performance of the reduced model is shown in dashed-dotted lines in Fig. 15, in which the solid lines represent the dynamics from the original model. By analyzing generator rotor angle data from the time interval of $1.2\mathrm{s} < t < 5\mathrm{s}$, generators G2, G4, G5, and G7 at Bus 36 are identified as characteristic generators; generators

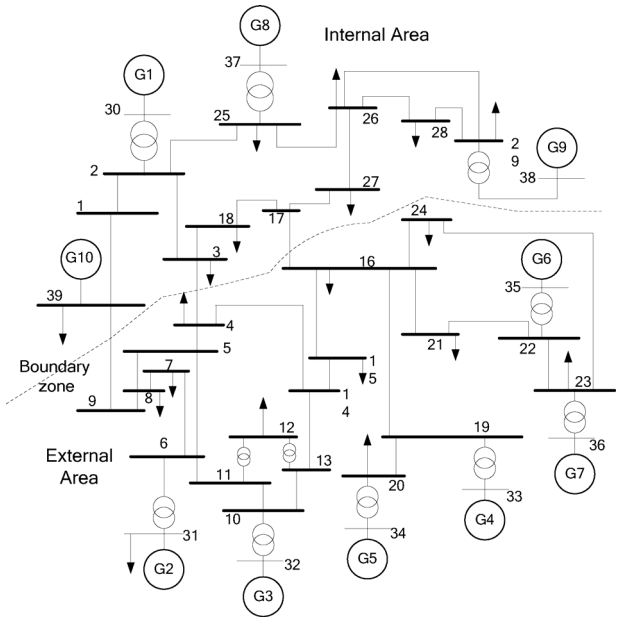

Fig. 14. Diagram of the IEEE 39-bus system.

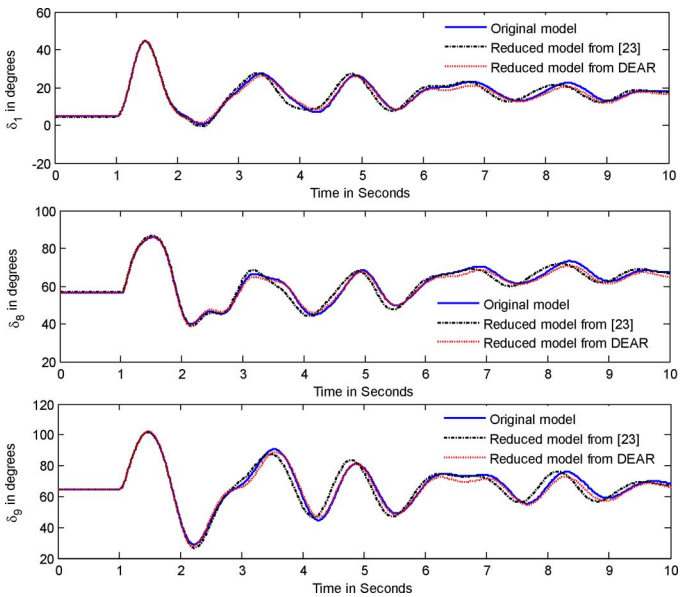

Fig. 15. Dynamic response of internal generators in the IEEE 39-bus system (Generator 10 at Bus 39 is chosen as a reference).

TABLE III
ERROR FUNCTIONS FROM (22) AND (23) FOR MACHINES G1 AT BUS 30, G8 AT BUS 37, AND G9 AT BUS 38 IN THE IEEE 39-BUS SYSTEM

Reduction Method	$J_a(1)$	$J_s(1)$	$J_a(8)$	$J_s(8)$	$J_a(9)$	$J_s(9)$
Method in [23]	1.531	1.941	1.712	2.187	2.831	3.753
DEAR method	0.840	1.034	0.965	1.192	1.438	1.229

G3 and G6 at Bus 35 are replaced by the linear combination of the above characteristic generators. Under the same reduction ratio, the performance of the DEAR method is shown as the dotted lines in Fig. 15. Using the metrics in (22) and (23), the errors of the reduced models are given in Table III. As can be seen from Table III, the proposed method shows a better performance than the coherency-based method.

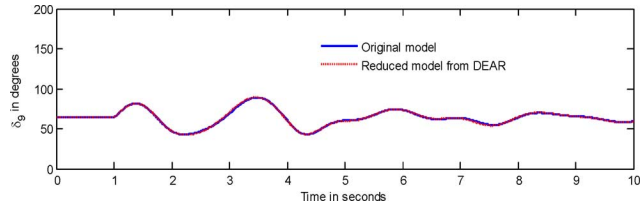

Fig. 16. Dynamic response of Generator 9 under fault duration of 40 ms.

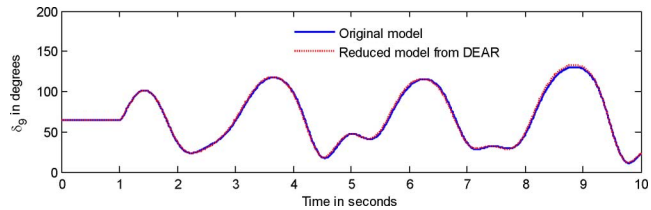

Fig. 17. Dynamic response of Generator 9 under fault duration of 70 ms.

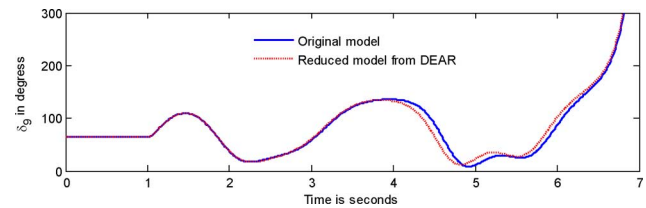

Fig. 18. Dynamic response of Generator 9 under fault duration of 80 ms.

To test the performance of the proposed method under the scenario of system instability, a three-phase fault at Bus 26, which lasts for 40 ms, 70 ms and 80 ms, respectively, is cleared by removing the line between Bus 26 and Bus 25. Figs. 16–18 show the responses under different fault durations. The system goes from stable to unstable as fault duration increases.

As can be seen from Figs. 16–18, the reduced model can track the trajectories of the original model very well in both stable and unstable scenarios.

To test the performance under first swing instability scenarios, we configured a three phase short circuit fault at Bus 30 (the terminal bus of G1). After the fault being cleared, the line between bus 30 and bus 2 trips and G1 disconnects from the system. Fig. 19 shows the performance of the reduced model in this scenario. As can be seen from Fig. 19, trajectories of the reduced model and the original model can still match well.

Another test was set up to check the performance under marginal stability scenarios. We added one more line[4] between Bus 2 and Bus 30 shown in Fig. 20, so that after one line is tripped following the three phase short circuit fault, the other line still keeps G1 connected. The system is unstable if the fault lasts for 270 ms, which is shown by the dash line (rotor angle difference between G1 and G9) in Fig. 21. The solid line in Fig. 21 is the response when the fault lasts for 240 ms, which is considered as a marginal stability scenario. The performance of the reduced model under the marginal stability scenario is shown in Figs. 22 and 23. The response curves still match well, although the mismatches look larger than Figs. 16–19.

[4]The added line has the same parameters as the existing one.

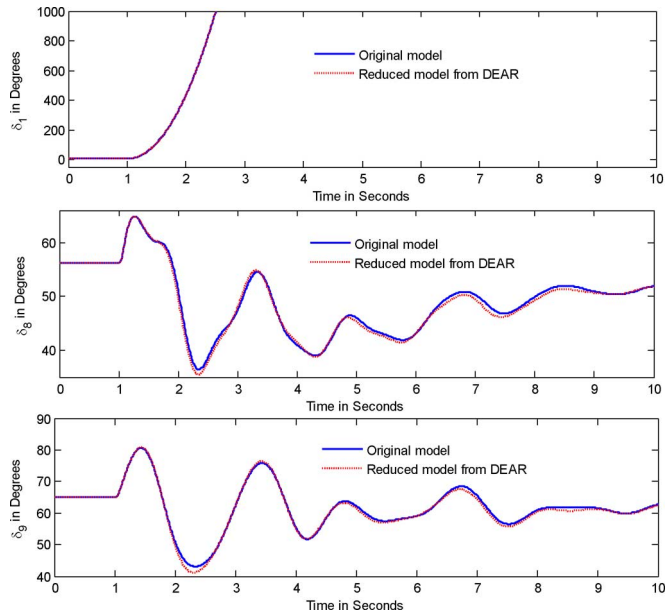

Fig. 19. Performance under the first swing instability (Generator 10 at Bus 39 is chosen as a reference).

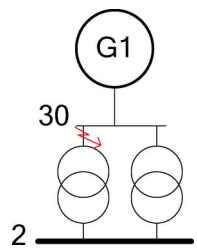

Fig. 20. Double-line connection between Bus 30 and Bus 2.

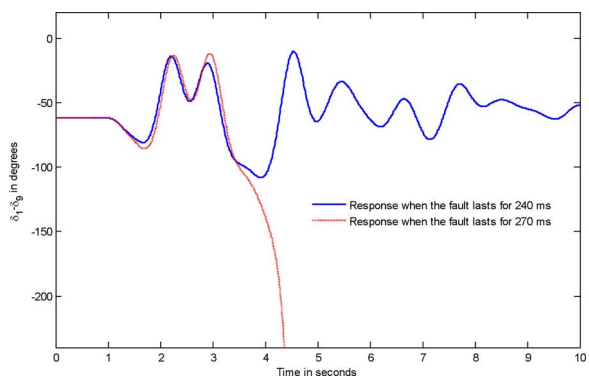

Fig. 21. Scenarios of marginal stability and instability.

V. Conclusions

A measurement-based dynamic model reduction method that simplifies the external (target) systems through dynamic-feature extraction, attribution, and reconstruction is proposed. The new method is named DEAR method. The network model is unchanged in the DEAR method, which makes online applications relatively easier and more flexible (e.g., generators of interest can be retained in the reduced model). Tests on several IEEE standard systems show that the DEAR method yields better reduction ratios and smaller response errors than the traditional coherency-based aggregation methods. The paper also shows that the DEAR method works well under stable, marginally stable and unstable conditions.

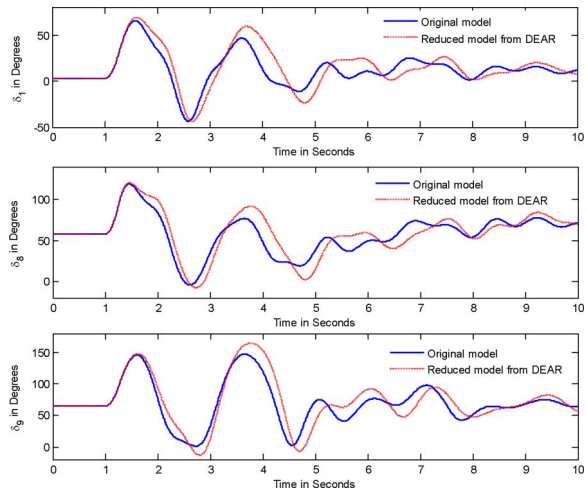

Fig. 22. Response of rotor angles in the scenario of marginal stability (Generator 10 at Bus 39 is chosen as a reference).

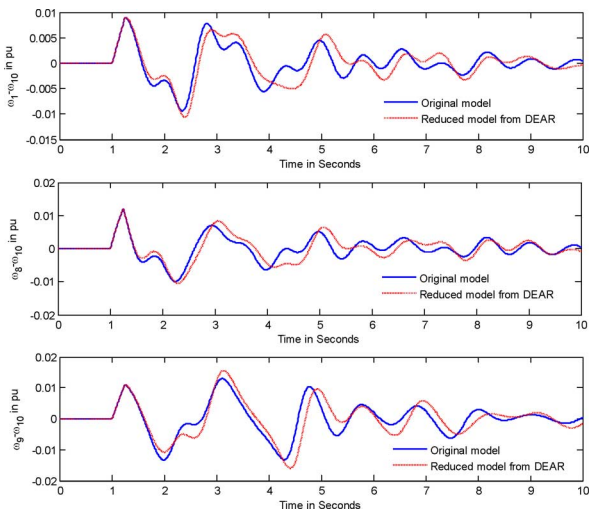

Fig. 23. Response of rotor speeds in the scenario of marginal stability (Generator 10 at Bus 39 is chosen as a reference).

This paper also demonstrates the online application of DEAR method using a super set of characteristic generators and online refinement of the coefficient matrix through a simple case. Performance of the reduced model under both stable and unstable conditions is verified. Further investigation on the robustness of the method against fault locations, topology and operation point changes will be carried out in the future work.

Acknowledgment

The authors would like to thank Prof. J. H. Chow for his help in performance comparison of different model reduction methods.

References

[1] F. Ma and V. Vittal, "Right-sized power system dynamic equivalents for power system operation," *IEEE Trans. Power Syst.*, vol. 26, no. 4, pp. 1998–2005, Nov. 2011.

[2] R. Podmore, "Identification of coherent generators for dynamic equivalents," *IEEE Trans. Power App. Syst.*, vol. PAS-97, no. 4, pp. 1344–1354, Jul./Aug. 1978.
[3] S. E. M. d. Oliveira and A. G. Massaud, "Modal dynamic equivalent for electric power systems. II. Stability simulation tests," *IEEE Trans. Power Syst.*, vol. 3, no. 4, pp. 1731–1737, Nov. 1988.
[4] S. E. M. d. Oliveira and J. F. d. Queiroz, "Modal dynamic equivalent for electric power system. I. Theory," *IEEE Trans. Power Syst.*, vol. 3, no. 4, pp. 1723–1730, Nov. 1988.
[5] J. Chow, P. Accari, and W. Price, "Inertial and slow coherency aggregation algorithms for power system dynamic model reduction," *IEEE Trans. Power Syst.*, vol. 10, no. 2, pp. 680–685, May 1995.
[6] S. B. Yusof, G. J. Rogers, and R. T. H. Alden, "Slow coherency based network partitioning including load buses," *IEEE Trans. Power Syst.*, vol. 8, no. 3, pp. 1375–1382, Aug. 1993.
[7] X. Lei, D. Povh, and O. Ruhle, "Industrial approaches for dynamic equivalents of large power systems," in *Proc. IEEE Power Eng. Society Winter Meeting*, Jan. 27–31, 2002, vol. 2, pp. 1036–1042.
[8] K. K. Anaparthi, B. Chaudhuri, N. F. Thornhill, and B. Pal, "Coherency identification in power systems through principal component analysis," *IEEE Trans. Power Syst.*, vol. 20, no. 3, pp. 1658–1660, Aug. 2005.
[9] N. Senroy, "Generator coherency using the Hilbert–Huang transform," *IEEE Trans. Power Syst.*, vol. 23, no. 4, pp. 1701–1708, Nov. 2008.
[10] M. L. Ourari, L.-A. Dessaint, and V.-Q. Do, "Dynamic equivalent modeling of large power systems using structure preservation technique," *IEEE Trans. Power Syst.*, vol. 21, no. 3, pp. 1284–1295, Aug. 2006.
[11] J. P. Yang, G. H. Cheng, and Z. Xu, "Dynamic reduction of large power system in PSS/E," in *Proc. IEEE/PES Transmission and Distribution Conf. and Exhibition: Asia and Pacific*, Dalian, Liaoning, China, Aug. 18–18, 2005.
[12] G. N. Ramaswamy, G. C. Verghese, L. Rouco, C. Vialas, and C. L. DeMarco, "Synchrony, aggregation, and multi-area eigenanalysis," *IEEE Trans. Power Syst.*, vol. 10, no. 4, pp. 1986–1993, Nov. 1995.
[13] G. N. Ramaswamy, C. Evrard, G. C. Verghese, O. Fillatre, and B. Lesieutre, "Extensions, simplifications, and tests of synchronic modal equivalencing (SME)," *IEEE Trans. Power Syst.*, vol. 12, no. 2, pp. 896–905, May 1997.
[14] S.-K. Joo, C.-C. Liu, L. E. Jones, and J.-W. Choe, "Coherency and aggregation techniques incorporating rotor and voltage dynamics," *IEEE Trans. Power Syst.*, vol. 19, no. 2, pp. 1068–1075, May 2004.
[15] S. Wang, S. Lu, G. Lin, and N. Zhou, "Measurement-based coherency identification and aggregation for power systems," in *Proc. IEEE PES General Meeting*, San Diego, CA, USA, Jul. 22–26, 2012.
[16] R. Singh, M. Elizondo, and S. Lu, "A review of dynamic generator reduction methods for transient stability studies," in *IEEE Power and Energy Society General Meeting 2011*, Detroit, MI, USA, Jul. 24–29, 2011.
[17] B. Moore, "Principal component analysis in linear systems: Controllability, observability, and model reduction," *IEEE Trans. Autom. Control*, vol. AC-26, no. 1, pp. 17–32, Feb. 1981.
[18] C. A. Cañizares, N. Mithulananthan, F. Milano, and J. Reeve, "Linear performance indices to predict oscillatory stability problems in power systems," *IEEE Trans. Power Syst.*, vol. 19, no. 2, pp. 1104–1114, May 2004.
[19] S. Liu, "Dynamic-data driven real-time identification for electric power systems," Ph.D. dissertation, Dept. Elect. Eng., Univ. Illinois, Urbana-Champaign, Urbana, IL, USA, 2009.
[20] K. Glover, "All optimal Hankel norm approximation of linear multivariable systems, and their L^∞-error bounds," *Int. J. Control*, vol. 39, no. 6, pp. 1145–1193, 1984.
[21] D. P. Berrar, W. Dubitzky, and M. Granzow, *A Practical Approach to Microarray Data Analysis*. Norwell, MA, USA: Kluwer, pp. 91–109.
[22] A. C. Antoulas, *Approximation of Large-Scale Dynamical Systems*. Philadelphia, PA, USA: SIAM, 2005.
[23] G. Pyo, J. Park, and S. Moon, "A new method for dynamic reduction of power system using PAM algorithm," in *Proc. IEEE PES General Meeting*, Minneapolis, MN, USA, Jul. 25–29, 2010.
[24] North American Electric Reliability Corporation (NERC) Transmission Operation (TO) and Transmission Planning (TPL) Standards [Online]. Available: http://www.nerc.com/page.php?cid=2%7C20

Shaobu Wang (M'12) received the Ph.D. degree in electrical engineering from Zhejiang University, Hangzhou, Zhejiang province, China, in 2009.

From March 2009 to March 2010, he worked as a postdoctoral fellow in the Department of Electrical and Computer Engineering, University of Alberta, Edmonton, AB, Canada. From April 2010 to April 2011, he worked as a postdoctoral research associate in the Center for Energy Systems Research, Tennessee Technological University, Cookeville, TN, USA. From May 2011 to July 2011, he worked as a research scholar in the Department of Electrical and Computer engineering, University of Denver, Denver, CO, USA. He is currently with Pacific Northwest National Laboratory, Richland, WA, USA. His research interests include PMU-based monitoring and control of power systems and renewable energy integration.

Shuai Lu (M'06–SM'13) received the B.S. and M.S. degrees from Tsinghua University, China, and the Ph.D. degree from the University of Washington, Seattle, WA, USA, all in electrical engineering.

He is a senior research engineer at Pacific Northwest National Laboratory (PNNL). He has led power system R&D projects at PNNL on renewables integration, operation modeling, dynamic security, and demand response. Prior to joining PNNL in 2006, he conducted research on the design of undersea power and communication networks, and developed digital controllers and models for voltage control devices.

Ning Zhou (S'01–M'05–SM'08) received the Ph.D. degree in electrical engineering with a minor in statistics from the University of Wyoming, Laramie, WY, USA, in 2005.

He is an Assistant Professor at the Electrical and Computer Engineering Department of the Binghamton University. He was with Pacific Northwest National Laboratory (PNNL) as a power system engineer from 2005 to 2013. His research interests include power system dynamics and statistical signal processing.

Dr. Zhou is a senior member of the IEEE Power and Energy Society (PES)

Guang Lin (M'12) received the B.S. degree in mechanics with a minor in electrical engineering from Zhejiang University, China, in 1997; the M.S. degree in mechanics and engineering science from Peking University, China, in 2000; and the M.S. and Ph.D. degrees in applied mathematics from Brown University, Providence, RI, USA, in 2004 and 2007, respectively.

He is a senior research scientist at Pacific Northwest National Laboratory. He has had in-depth involvement in developing uncertainty quantification tools for a large variety of domains including energy and environment. His research interests include diverse topics in computational science both on algorithms and applications, uncertainty quantification, large-scale data analysis, and multiscale modeling in a large variety of domains.

Dr. Lin is currently serving on the editorial board of the *International Journal for Uncertainty Quantification*.

Marcelo Elizondo (S'98–M'07) received the Electrical Engineer degree in power systems from Universidad Nacional de San Juan, Argentina, in 2001; and the Ph.D. degree in power system engineering from Universidad Nacional de San Juan, Argentina, in 2008.

In 2001 he was an undergraduate visiting scholar at Supélec, France; from 2003 to 2005, he was a graduate visiting scholar at Carnegie Mellon University, Pittsburgh, PA, USA. He worked in Mercados Energéticos Consultores (Argentina), an international power system consulting firm, from 2007 to 2009. He has been a Research Engineer at Pacific Northwest National Laboratory since 2009. His current research interests include power system dynamic modeling and analysis in transmission, distribution, and microgrids; operation and control of HVdc systems; and technical and commercial aspects of international power system interconnections.

M. A. Pai (LF'96) received the B.S. degree from the University of Madras, Madras, India, in 1953 and the M.S. and Ph.D. degrees from the University of California Berkeley in 1958 and 1961, respectively.

He was with the faculty of the Indian Institute of Technology, Kanpur, India, from 1963 to 1981. From 1981 to 2003, he was with the faculty of the University of Illinois at Urbana-Champaign, where he is currently Professor Emeritus in the Department of Electrical and Computer Engineering.